A Model-Free Extremum-Seeking Approach to Autonomous Excavator Control Based on Output Power Maximization

A Model-Free Extremum-Seeking Approach to Autonomous Excavator Control Based on Output Power Maximization*

Filippos E. Sotiropoulos and H. Harry Asada, *Member, IEEE*

***Abstract*—A new approach to autonomous excavator control that allows the machine to adapt to unknown soil properties is presented. Unlike traditional force control or trajectory control, the new method uses the product of force and velocity, namely, the power transmitted from the excavator to the soil, as a signal for adaptive excavation. Using an extremum-seeking algorithm, an optimal excavation condition where the force and velocity at the bucket take a particular combination that maximizes the output power of the machine is sought and maintained. Under this condition, the system finds the optimal depth of digging by controlling the boom of the excavator. Also under this condition, the output impedance of the excavator matches the impedance of the load and, thereby, transmits the maximum power from the machine to the soil. Theoretical analysis proves that an optimal combination of force and velocity exists and is unique under mild assumptions. An extremum-seeking algorithm using recursive least squares is developed for maximizing the output power. The method is implemented on a small-scale prototype system where torque motors emulate nonlinear force-speed characteristics of hydraulic actuators. Experiments demonstrate that the prototype can execute excavation tasks adaptively against varying soil properties and terrain profile.**

***Index Terms*—Mining Robotics, Robotics in Construction, Field Robots, Extremum-Seeking Control**

I. Introduction

There is a worldwide shortage of skilled operators who can operate excavators and other earth moving equipment effectively and productively. Excavators, as shown in (Fig. 1), are the key equipment in construction and mining industries, which have shown a rapid growth in the last few decades. The world market of the construction industry alone is over $8 trillion, which is predicted to reach over $10 trillion by 2020 [1]. Training excavator operators takes a long time and requires a significant amount of investment. The work environment of excavation is often harsh and dangerous, leading to difficulties in recruitment and low retention rate. Large-scale mining sites, in particular, are sometimes located in the middle of a desert or an isolated place - an unpleasant environment for operators to stay. Thus, the industries have been facing a severe shortage of skilled operators, which is pervasive worldwide and hampering the growth of the industries. Therefore, the construction and mining equipment industry has been investigating the development of autonomous excavators as a solution to these challenges. Excavators deal with soil and rocks, which are distinctly more complex and challenging to manipulate than typical discrete objects that the majority of robots deal with. Soil and rocks are highly nonlinear, distributed, and time-varying. The terrain profile and properties of excavation sites are uncertain, unstructured, and non-uniform. Furthermore, the excavation machines themselves have complicated hydraulic circuits which exhibit significant nonlinear dynamics. Through years of experience, skilled operators of excavators are capable of handling all these factors in making control and task planning decisions for a wide set of situations.

*This work was supported by Komatsu Ltd.

F. E. Sotiropoulos (fes@mit.edu) and H. H. Asada (asada@mit.edu) are with the Department of Mechanical Engineering, Massachusetts Institute of Technology, 77 Massachusetts Ave., Cambridge, USA. (The corresponding author is F. E. Sotiropoulos).

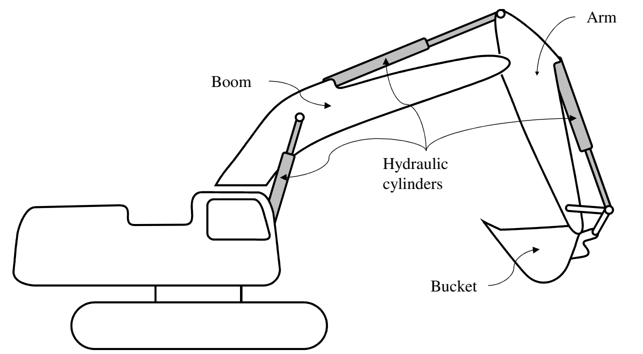

Fig. 1. Schematic showing the essential elements of a typical hydraulic excavation machine. The three arm linkages and their respective hydraulic actuators are indicated.

Despite various research efforts over the last three decades, autonomous control has fallen short of providing an adequate replacement for the efficacy and versatility of a well-trained human operator. There are numerous challenges in the field of earthmoving autonomy [2] which must be tackled in developing a completely autonomous system. One of the most prominent issues is trajectory planning and real-time control that adequately deal with tool-soil interactions. The first efforts in autonomous digging were mostly a geometric approach to planning trajectories [3]. Trajectory profiles were parametrized and designed so as to fulfill objectives on soil volume excavated and meet kinematic constraints imposed by the machine. Interactions between the bucket and soil are considered by using simple soil models such as the Fundamental Equation of Earthmoving [4] (FEE) and identifying the pertinent soil parameters. While the FEE assumes a flat blade moving horizontally through the soil, efforts were made to expand the applicability to sloped soil [5] and to include the increasing accumulated soil in front of the blade [6]. Furthermore, many other models have been proposed for predicting digging forces; some of these are well summarized in [7].

Real-time feedback control that can adapt to varying soil conditions has been studied by many groups. Some of the earliest work on robotic excavation by Bernold [8] proposed impedance control [9] as a potential method for controlling the relationship between the path of the bucket and the resistive force encountered during digging. It was observed that, given a nominal desired trajectory, the excavator follows a modified trajectory depending on the resistive force from the soil. This was applied and extended by Maeda and Rye [10] to prevent excessively high forces from being generated at the bucket. The desired terrain geometry is reached through iterative digging. A related but differing approach was pursued by Dobson, Marshall and Larsson [11] where the converse of impedance control was investigated. An admittance-based controller was implemented on a haul-loader which set the demand velocity on the curl cylinder in response to measured reaction forces. The method showed that admittance control can achieve high levels of productivity and consistency for front loaders. Another force feedback method was recently proposed by Jud et al. [12]. In their method an explicit desired force trajectory is prescribed with lower priority being allocated to the bucket path. Through simulation the authors showed that this results in trajectories which are distinctly different depending on the soil characteristics and are similar to the changes an expert operator may take.

For the purpose of designing trajectories and control synthesis, terramechanics and soil-bucket interactions have been studied. However, simple models fail to predict critical phenomena, resulting in unreliable prediction, while more complex models such as Discrete Element Modeling (DEM) are prohibitively complex and too computationally expensive for real-time applications. Furthermore, all models rely on detailed knowledge of the environment which is not possible to attain. In general, model based methods are difficult to apply to unknown and varying terramechanic conditions.

In the current work, a different approach is pursued. Instead of setting a desired force as well as setting particular impedance, admittance, or compliance values, this method aims to maximize a particular metric that is computable through direct measurements. Specifically, this method maximizes the product of force and velocity, that is, power transmitted from an excavator to the soil. Finding a desired value for force, impedance, admittance, etc. requires both soil and excavator properties. Since we can directly measure both force and velocity, this power maximization approach does not need explicit properties of the machine and the soil. Therefore, it is model-free. Furthermore, the power transmission depends on both soil and machine properties. As such, this approach integrates both properties into a simple scalar metric and allows the system to adapt to changes to both properties.

II. Expert Operations

Prior to explaining the details of the proposed control algorithm, a brief description about excavator operations while digging a ditch is presented. According to standard training manuals of excavators in industry and excavator control literature [13], the operation of an excavator can be split into three distinct phases. As illustrated in Fig. 2, the digging operation of a standard trench-shaped ditch is performed in three distinct phases: penetrate, drag, and scoop motions. The role of the penetration phase is to pierce the soil surface and let the bucket reach an effective digging depth and cutting angle (the angle of the bucket with respect to the soil surface). This is followed by a relatively flat motion where the bucket moves forward, causing soil ahead of it to mechanically fail through shear and accumulate inside and in front of the bucket. The effective depth and direction of the bucket vary depending on the properties of the soil and the capacity of the machine. The final phase, scooping, is to collect the accumulated soil into the bucket so that it can be transfered to a destination.

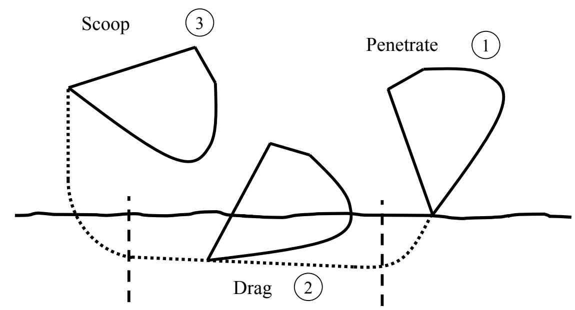

Fig. 2. The typical phases in a digging cycle. This includes (1) penetrate, (2) drag and (3) scoop. The second phase, dragging, often varies in length depending on the characteristics of the soil.

Based on literature [8], [12], [13] and observation of expert operators, we can find that each phase of digging is performed by coordinating particular links of an excavator:

- In the penetration phase, the arm (see Fig. 1) moves downwards providing thrust into the soil, and the boom also moves if necessary (depending on the soil geometry) to ensure the insertion of the bucket into the soil. The bucket (if placed in the correct orientation on approach) does not need to move and, in fact, its movement is generally restricted.
- In the dragging phase, the arm moves forward towards the cab. The boom moves so as to adjust the bucket trajectory, in particular, the depth of cut and direction of cut with respect to the soil surface. The boom movement affects the resistance encountered at the bucket. The bucket linkage remains locked, making only very small adjustments if necessary. The arm is the most active link and moves only forward. It does the majority of the work in the dragging phase.
- The final scooping phase is distinctly different from the preceding phases. Here the main action comes from the bucket, which curls upward to collect the soil moved in the previous phases. The boom and arm mainly act to prevent the soil from spilling out.

From the movements of each digging phase several points may be noted. The first is that throughout the digging phases all ordinary trajectories require the arm actuator to move only in one direction: forward. The majority of fine adjustment to the bucket tip position is performed with the boom control.

Secondly, the motion of the swing is not included in the majority of ordinary digging trajectories. For this reason, swing is generally ignored in most prior works on autonomous excavation and is also omitted in this work.

Finally, among the three phases the dragging phase needs a high level of operator skills. The boom must be controlled so that an excessively large force may not work on the bucket. The arm should not get stuck, but move forward at an adequate speed despite unpredictable changes to soil properties and other conditions. For this reason we focus on the dragging phase in this letter, and aim to develop a control algorithm that emulates an expert's operation in dragging.

According to expert operators during interviews, one of the key operational skills is to match the capacity of the machine with the load of soil. The bucket must move forward consistently through the soil. This can be achieved with appropriate boom control. Interestingly, experts never talked about a set-point velocity and desired force/pressure, but emphasized the match between the machine's capacity and the load. With the boom control, the load can be adjusted and matched with the machine's capacity. This can be interpreted as a type of impedance matching where a large amount of mechanical power is transmitted to the soil. The expert has the skill to achieve this condition with skillful operations of control levers.

This expert statement makes sense from the physical viewpoint. Essentially, the dragging phase is successive failure of the soil (primarily in the shear mode) [4], [7], [14]. This requires a large amount of energy to be transmitted to the soil so that the bucket can overcome cohesion and friction forces. Maximizing power output to the soil may result in the most productive usage of the machine to remove soil because the maximum amount of energy is made available for soil interactions.

In the method proposed in this letter, the motion of the excavator is updated in real-time so as to achieve a trajectory which maximizes power transmitted to the soil. This is achieved by using extremum-seeking control [15] to converge on an optimal operation point. Similarly to what is seen in the operation of excavators by skilled operators, this results in distinctly different trajectories depending on the characteristics of the environment [13]. The method does not depend on a model of the environment or machine, but instead uses two sensed quantities (speed and force). This allows the controller to compensate for varying conditions of the environment and machine, resulting in consistent digging motions which maximize work done on the soil.

III. Power Maximization Extremum-Seeking

A. Power Maximization Problem Statement

Hydraulic actuators, present in excavators, exhibit force-speed characteristics similar to that conceptually sketched in Fig. 3. The operational state of the machine is dependent on the load acted upon. Depending on the depth of the bucket, the load due to the soil varies and, thereby, the force exerted by the arm actuator and its speed change. At one limit, if the boom directs the bucket to go very deep into the soil, the arm actuator may stall, thus exerting a maximum force, but zero speed. At the other extreme, the bucket is barely touching the soil or placed very shallowly into the soil. In this case, the force on the arm actuator is very low and the speed is very high being limited by the internal resistance of the machine. In both of these limit cases, the power transmitted from the arm actuator is minimum. In between lies an operating condition where the bucket moves consistently through the soil with adequate force and speed, exerting the maximum power through the arm cylinder. As detailed in following sections of this paper, a method is proposed where the state of maximum power transfer is chosen as the desired state. As stated previously, the goal is to maximize the work per unit time (P_s) delivered to the soil during the dragging phase such that soil shear failure continues to occur.

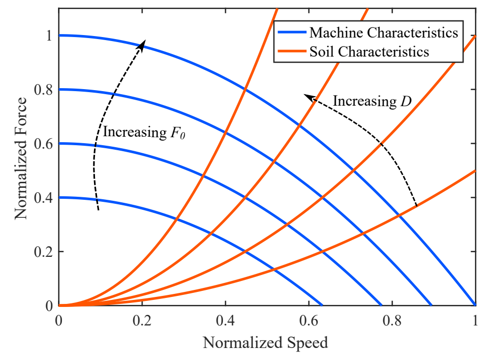

Fig. 3. Conceptual sketch of force characteristics of hydraulic machine and soil characteristics.

$$P_s = F_a v_a \tag{1}$$

where F_a is the force acting on the bucket in the direction of the arm movement, and v_a is the bucket velocity in the same direction. Several assumptions when formulating the problem are made on the above work expression:

- The power due to the boom motion is ignored;
- The bucket is fixed during the dragging phase; and
- The process is quasi-static.

The force-speed characteristics of the arm's hydraulic actuator is described by a nonlinear function, g_m:

$$F_m = g_m(v_a, F_0) \tag{2}$$

where F_m is the output force of the hydraulic cylinder, (pump supply pressure) $\times$ (cross-sectional area of the cylinder), and F_0 is its value at zero speed, called a stall force. The nonlinear function $g_m(v_a, F_0)$ is assumed to be continuously differentiable.

The soil resistive characteristics are expressed as:

$$F_a = f_a(v_a, D) \tag{3}$$

where D is the bucket depth of cut. The nonlinear function $f_a(v_a, D)$ is assumed to be continuously differentiable. Also, the force becomes zero for zero depth of cut: $F_a = 0$, for $D = 0$. For these force-speed characteristics we further assume the following:

Assumption 1. *The force-speed characteristics of hydraulic actuators are non-positive in its partial derivative with respect to v_a:*

$$\frac{\partial g_m}{\partial v_a} \leq 0, \quad \forall F_0 > 0 \tag{4}$$

Assumption 2. *The output power of the hydraulic actuator given by*

$$P_m = F_m v_a \tag{5}$$

is convex with respect to v_a when the actuator is subject to the force-speed characteristics (2). The maximum of actuators output power is therefore unique.

Assumption 2 holds for many actuator types, including hydraulic actuators and electric motors.

Assumption 3. *The soil characteristic equation, $F_a = f_a(v_a, D)$, is a monotonically increasing function of depth D for an arbitrary positive v_a :*

$$\frac{\partial f_a}{\partial D} > 0, \quad \forall v_a \in (0, v_{a,\max}) \tag{6}$$

and is also a monotonically increasing function of v_a for an arbitrary D:

$$\frac{\partial f_a}{\partial v_a} > 0, \quad \forall D \in (0, D_{\max}) \tag{7}$$

Fig. 3 illustrates the force-speed characteristics of a typical hydraulic actuator and that of soil load that satisfy the above assumptions.

B. Power Maximization as an Extremum-Seeking Problem

We aim to maximize the power delivered to soil by using an extremum-seeking algorithm. The work delivered to soil per unit time cannot exceed the maximum output power of the actuator, $P_{m,max}$:

$$P_s \le P_{m,max} \tag{8}$$

Let (v_a^o, F_m^o) be the pair of actuator speed and force that maximizes the actuator output power:

$$(v_a^o, F_m^o) = \underset{v_a, F_m}{\arg\max}\, P_m \tag{9}$$

Because of the convexity assumption of the actuator output power, the maximum power pair (v_a^o, F_m^o) is unique. Note that the actuators speed and force are not only dependent on its own characteristics, but are also determined by the load; that is, the soil characteristics. The resistive force F_a varies depending on the depth of cut D. Now we can show that, under mild conditions, there exists an optimal depth of cut D^o providing an optimal load and that the optimal depth is unique.

C. Existence of an Optimal Point

Since the process is quasi-static, inertial forces are ignored. Therefore, the output force of the arm actuator balances the force acting on the bucket in the same direction:

$$F_m = F_a \tag{10}$$

Therefore,

$$h(D, F_0, v_a) \equiv f_a(v_a, D) - g_m(v_a, F_0) = 0 \tag{11}$$

Differentiating the above with respect to v_a, we obtain that

$$\frac{\partial}{\partial v_a} h(D, F_0, v_a) = \frac{\partial}{\partial v_a} f_a(v_a, D) - \frac{\partial}{\partial v_a} g_m(v_a, F_0) \neq 0 \tag{12}$$

since

$$\frac{\partial f_a}{\partial v_a} > 0, \quad \forall D \in (0, D_{\max}) \quad \text{and} \quad \frac{\partial g_m}{\partial v_a} \le 0, \quad \forall F_0 > 0. \tag{13}$$

From the implicit function theorem, there exists an explicit function relating v_a to D:

$$v_a = \phi(D, F_0), \quad \forall D \in (0, D_{\max}),\ \forall F_0 > 0 \tag{14}$$

Lemma 1. *Given a constant F_0, we can show that:*

$$\frac{\partial \phi}{\partial D} < 0 \tag{15}$$

Proof. From the total derivative of function $h(D, F_0, v_a)$ we can obtain

$$\frac{\partial f_a}{\partial v_a} dv_a + \frac{\partial f_a}{\partial D} dD - \frac{\partial g_m}{\partial v_a} dv_a = 0 \tag{16}$$

since F_0 is constant. Therefore, from assumptions 1 and 3

$$\frac{\partial v_a}{\partial D} = -\frac{\frac{\partial f_a}{\partial D}}{\frac{\partial f_a}{\partial v_a} - \frac{\partial g_m}{\partial v_a}} < 0. \tag{17}$$

■

Suppose that the maximum power pair (v_a^o, F_m^o) satisfies the soil characteristic equation,

$$F_m^o = f_a(v_a^o, D), \tag{18}$$

where the pair also satisfies,

$$F_m^o = g_m(v_a^o, F_0) \tag{19}$$

From the implicit function theorem, these two conditions reduce to

$$v_a^o = \phi(D, F_0) \tag{20}$$

If the stall force F_0 is chosen such that the above algebraic equation has a solution for D, then the depth of cut that provides the machine with the optimal load is unique because the function $\phi(D, F_0)$ is a monotonically decreasing function of D, from Lemma 1. At this particular depth of cut D^o the load of the soil gives the optimal combination (v_a^o, F_m^o), which is to deliver the maximum power to the soil:

$$P_{s,max} = P_{m,Max} = v_a^o F_m^o \ge v_a F_m. \tag{21}$$

In other words, the output impedance of the actuator matches the load impedance. All we need to do is to control D via the boom motion so that the actuators output power can become a maximum. This is an extremum-seeking problem. Note that we do not need a model of soil characteristics, nor the actuators force-speed characteristics. We have to assume the basic properties of functions f_a and g_m, but there is no need to know the profiles of the functions.

D. Extremum-Seeking Algorithm

Fig. 4 shows the output power P_s against the depth of cut D. The optimal dragging operation is achieved by seeking the peak of the output power by controlling the depth of cut. Extremum-Seeking Control (ESC) estimates the gradient of the output power curve, and controls the depth of cut via the control of the boom in the direction of the maximum output power.

The correction to boom trajectory must be made in such a way so as to increase the power output of the machine from the arm. As such, the ESC controller determines the local gradient of output power with respect to the boom position, x_b, and corrects using a proportional-integral adaptation law (Fig. 5). Classical ESC uses simply an integral adaptation law, but the

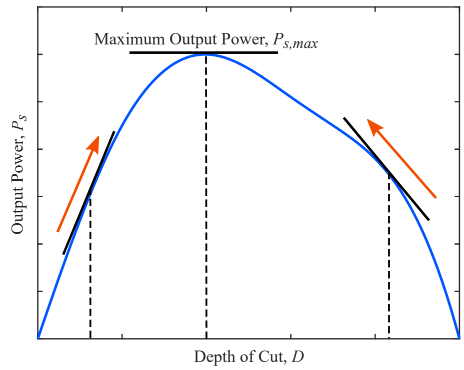

Fig. 4. The ESC algorithm guides the state of the machine to the peak power condition based on the estimated local gradient.

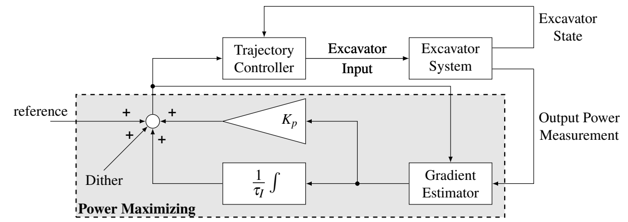

Fig. 5. High-level block diagram of the power maximizing algorithm utilizing ESC. The *Trajectory Controller* block accepts state measurements and the desired joint trajectory. It can take many forms, depending on the chosen implementation but implements the low level control of the robot. The *Gradient Estimator*, determines the local gradient of Output Power with respect to the tunable trajectory parameter. The integrator block and K_p gain term represent the trajectory adaptation law.

combination of a proportional term has been shown to improve transient performance [16], [17].

The recursive least squares algorithm with forgetting factor [18] is used to calculate the estimated local gradient $\hat{\theta}_1$ of power with respect to boom position. The gradient is determined by estimating the parameters, θ_0 and θ_1, of the simple estimator model:

$$P_m = \theta_1 x_b + \theta_0 \tag{22}$$

As such, the gradient estimator is given by:

$$\hat{\theta}(k) = \hat{\theta}(k-1) + \frac{\Sigma_{k-1}\xi(k)[P_m(k) - \xi^T(k)\hat{\theta}(k-1)]}{\alpha + \xi^T(k)\Sigma_{k-1}\xi(k)} \tag{23}$$

$$\Sigma_k = \frac{1}{\alpha}\left[\Sigma_{k-1} - \frac{\Sigma_{k-1}\xi(k)\xi^T(k)\Sigma_{k-1}}{\alpha + \xi^T(k)\Sigma_{k-1}\xi(k)}\right] \tag{24}$$

where k is the time step, $\hat{\theta}(k) = [\hat{\theta}_1(k), \hat{\theta}_0(k)]^T \in \mathbb{R}^{2\times1}$ is the estimated parameter vector at time k with $\hat{\theta}_1(k)$ being the local gradient as defined previously and $\hat{\theta}_0(k)$ is the offset. $P_m(k) \in \mathbb{R}$ is the arm power measurement at time k and $\xi(k) = \begin{bmatrix} x_b(k) & 1 \end{bmatrix}^T \in \mathbb{R}^{2\times1}$ is the regressor which is composed of the boom position and a constant unity term. $\Sigma_k \in \mathbb{R}^{2\times2}$ is the covariance matrix used for the parameter estimation at time k and α is the 'forgetting factor' which is set between 0 and 1.

The estimated gradient is then padded by zeros to make a new vector ψ, whose dimensions are consistent with the input to the low level controller $\mathbf{u}(k) = \begin{bmatrix} x_{1,d} & x_{2,d} & x_{3,d} \end{bmatrix}^T \in \mathbb{R}^{3\times1}$. The variables $x_{i,d}$ are the desired actuator positions for the low level controller where $i = 1,2,3$ represent the desired position trajectory for the boom, arm and bucket respectively.

$$\psi(k) = \begin{bmatrix} \hat{\theta}_1(k) & 0 & 0 \end{bmatrix}^T \in \mathbb{R}^{3\times1} \tag{25}$$

The input $\mathbf{u}(k)$ in discrete time can then be determined using the adaptation law:

$$\mathbf{u}(k) = K_p\psi(k) + \gamma(k) + \mathbf{d}(k) + \mathbf{r}(k) \tag{26}$$

$$\gamma(k) = \tfrac{1}{2\tau_I}[\psi(k) + \psi(k-1)] + \gamma(k-1) \tag{27}$$

where $K_p \in \mathbb{R}$ is the proportional ESC gain and $\tau_I \in \mathbb{R}$ is the ESC integration time constant. $\mathbf{d}(k)$ is the dither used to excite the system to be able to detect the local gradient. A sinusoidal dither is used which is equivalent to:

$$\mathbf{d}(k) = \begin{bmatrix} b_1\sin(\omega_1 k/\Delta t) & 0 & 0 \end{bmatrix}^T \in \mathbb{R}^{3\times1} \tag{28}$$

where $\omega_1 \in \mathbb{R}$ is the dither frequency, $b_1 \in \mathbb{R}$ is the dither amplitude and $\Delta t \in \mathbb{R}$ the sample time. $\mathbf{r}(k) \in \mathbb{R}^{3\times1}$ is the reference trajectory determined from a trajectory planner paired with the proposed algorithm.

Assumption 4. *The dither signals provide persistent excitation such that there exist constants $\rho_\phi > 0$ and $T > 0$ where:*

$$\frac{1}{T}\sum_{j=k}^{k+T-1}\xi\xi^T > \rho_\xi I, \qquad \forall k > T. \tag{29}$$

This is a typical persistence of excitation condition [18] and is practically met by either a sinusoidal or stochastic dither.

IV. Experimental Implementation

This algorithm was implemented on a small-scale robotic excavator in order to verify its feasibility and validate the effectiveness of the proposed scheme for autonomous excavation.

A. Experimental Setup

The experiment setup consists of a 3 degree-of-freedom electrically-powered excavation robot (Fig. 6). The robotic excavator is scaled approximately 1:11 compared to a mid-size excavator (Komatsu PC-200 excavator). The arm and boom of the robotic excavator are powered by two torque motors (90W Maxon EC90 flat brush-less DC motors) with 50:1 gear heads (Harmonic Drive). The bucket is actuated with an integrated motor (100W Dynamixel Pro Servo motor). The boom and arm motors are driven by Maxon Escon 50/5 motor drivers, while the bucket motor has an integrated driver. A micro-controller is used to implement the low-level feedback control of the joints. The reference point is communicated from a desktop computer running ROS [19] connected serially via USB. The power maximizing loop is implemented on the desktop computer. The earth environment is created by filling large containers with soil placed in front of the robot.

As discussed in section II, excavators have to perform distinct phases of operation. Accordingly, the robotic excavator is controlled based on three distinct modes of operation, as shown

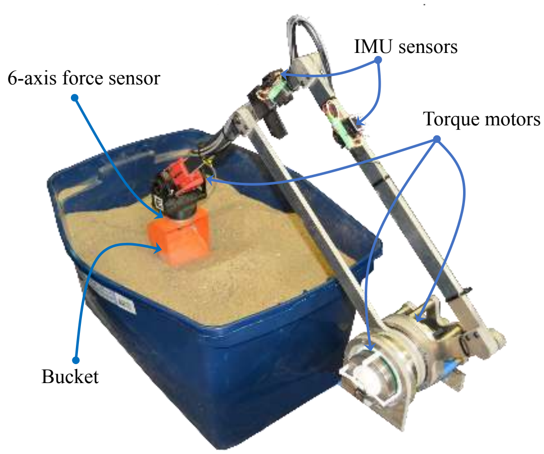

Fig. 6. Small scale excavation rig

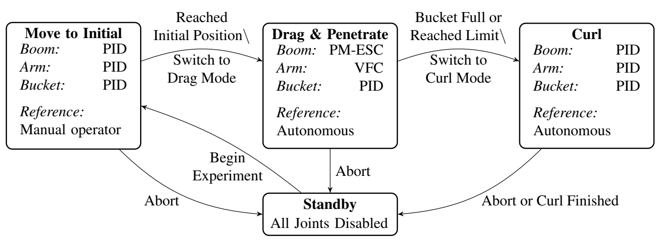

Fig. 7. Finite state machine representation of the mode switching between the different phases of the robot during the experiment. During each phase, the control mode of every joint and the reference point setting method is specified. PID represents a velocity PID controller, PM-ESC is the proposed algorithm and VFC represents the velocity feedback controlled simulated internal dynamics.

in Fig. 7. The operating mode and the transition conditions among them are encapsulated in the finite state machine. In this robotic excavation system, the first active phase, where the robot moves to the initial position, is performed manually. A human operator is to determine the starting point of digging, and the robot controller performs the rest of the cycle.

Various methods can be used for estimating the output power. For example, a torque and velocity measurement at the actuator would be the most direct measurement method. Directly measuring torque, however, is practically challenging; instead, the torque τ can be estimated by measuring the current of the motor i_{arm}. Then the torque is estimated using the motor torque constant K_T: $\tau = K_T i_{arm}$.

The result of power maximization depends on the force-speed characteristics of actuators. It is important to evaluate the algorithm for realistic actuator characteristics. To this end, the force-speed characteristics of a hydraulic cylinder are emulated by the torque motors with nonlinear velocity feedback. Namely, the torque motor is tuned to exhibit the following nonlinear torque-speed characteristics analogous to $F_a = g_m(F_0, v_a)$ as discussed in section III-A:

$$i_{arm} = g'_m(\tau_0, \omega_a) \tag{30}$$

where τ_0 is the stall torque and ω_a the arm speed. This can be linear or nonlinear, reflecting the resistance at valves and orifices. See Fig. 8. Figure 8(b) shows the quadratic relation that hydraulic valves exhibit.

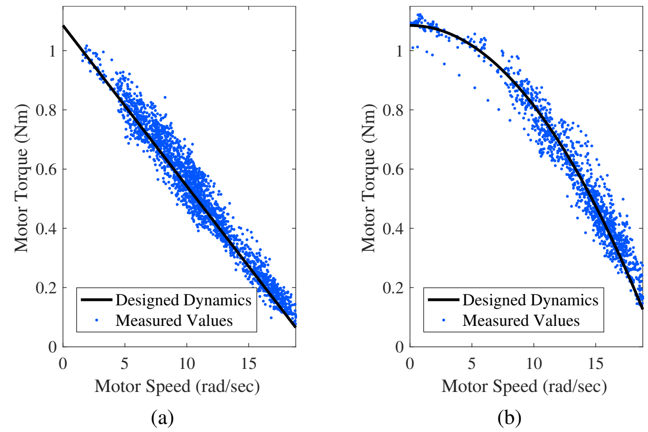

Fig. 8. Torque-Velocity characteristic of the arm actuator implemented to mimic a desired internal motor dynamics. Linear (a) and quadratic (b) speed to force characteristics are demonstrated.

In preliminary testing it was noted that both the depth, as well as its rate of change were significant in modulating soil resistance. Hence, the ESC algorithm was in fact implemented with respect to boom velocity.

V. Experiment

Experiments using the robotic excavator were conducted for diverse conditions. Specifically, the following tests were performed:

- Validation of Power Maximizing Extremum-Seeking Control (PM-ESC);
- Comparison to force control;
- Comparison of behaviors for hard and soft soil;
- Adaptation to changing soil properties;
- Bench geometry test;
- Multiple dig cycle trajectories.

The first test aims at establishing the efficacy of the extremum-seeking scheme to maximize the power consumed. This is achieved by comparing the PM-ESC controller to a force-feedback method. To have a like-for-like comparison of the algorithm, the force control is implemented in a similar architecture as the PM-ESC algorithm. In other words, the force control is implemented such that the force of the arm actuator is regulated by controlling the motion of the boom actuator:

$$v_{d,1} = PI(F_{arm,d}) \tag{31}$$

where $v_{d,1}$ is the velocity set point of the boom which is sent to the low level controllers and $PI(F_{arm,d})$ indicates a proportional-integral control law acting to track the desired reference force $F_{arm,d}$.

The other tests attempt to evaluate the effectiveness of the algorithm for excavation.

A. Experimental Test Results

In this section, the experimental results from the small-scale excavation rig are presented and discussed. For these tests, the linear internal impedance characteristic (Fig. 8a) was implemented.

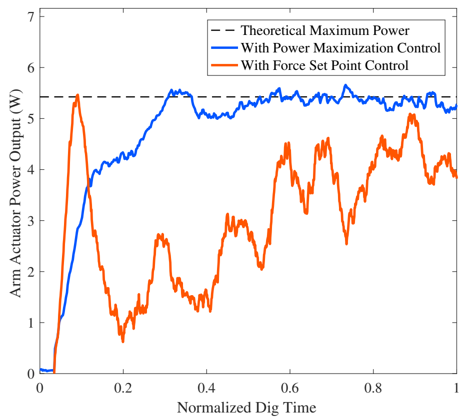

Fig. 9. Comparison of power output from arm actuator utilizing PMC and force feedback

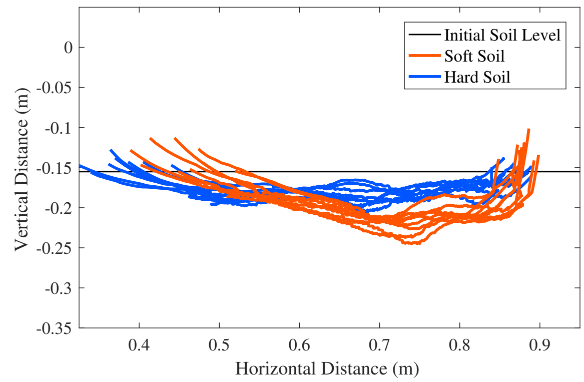

Fig. 10. Comparison of trajectories arising from the robot interacting with different soils. The softer soil (orange) results in deeper and shorter trajectories.

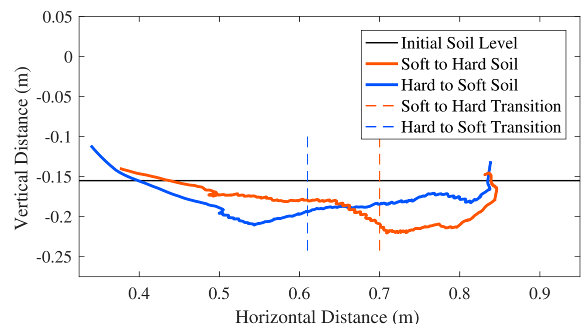

Fig. 11. Trajectories for the excavator moving through soil which changes properties abruptly. The dashed lines represent the point at which the soil hardness transitions.

1) Power Maximization Validation: In Fig. 9 one can compare the performance of the PM-ESC excavator control to the force control method tested on a flat soil surface. As can be seen, the PM-ESC reaches the machine maximum power state and remains in its vicinity. In contrast, the force control approach is considerably less consistent and power output varies more throughout the digging cycle. This shows how PM-ESC is effective at maintaining the machine close to the optimal operating condition.

2) Soil Hardness Comparison: One key challenge in excavation is that an autonomous excavator needs to deal with different soil properties and choose appropriate trajectories. The small scale excavation rig was tested on soils of different hardness. The first is a dry sand which offers lower resistance compared to the wet and compacted sand which it is compared to. A series of single dig cycles in each of the two environments are plotted in Fig. 10. As would be expected, the algorithm reacts to the different environments resulting in distinctly different digging trajectories which each operate closely to the maximum power state. The hard soil trajectories resemble the typical shallow 'penetrate-drag-scoop' while the softer soil trajectories take a deeper and shorter path (which is also the preferred method used by experts in loose soil). The soft soil trajectories, in fact, were on average $\sim 70\%$ deeper compared to the hard soil.

3) Soil Hardness Transition: A particular challenge in excavation is that the soil properties are highly changeable and can vary throughout an excavation cycle. A comparable situation is tested. A soil environment is established where there is a step change in hardness at some point in the horizontal direction. This is achieved by setting up the soil with a divider which is used during filling of the soil container. This is then slipped out prior to testing. The test is executed both for soil transitioning from hard-to-soft as well as soft-to-hard. The results from this can be seen in Fig. 11. For soft-to-hard, the penetration and initial drag is at a deep depth before quickly moving to a shallow depth once the hard soil is reached. The converse occurs for the hard-to-soft soil environment. Furthermore, Fig. 12 shows how after encountering the new soil type the power momentarily reduces, but then the adjustment in cutting depth restores a maximum power state promptly.

4) Bench Soil Geometry: It is often the case in excavation tasks that the machine has to remove soil from an angled soil surface known as a 'bench'. This scenario is replicated in experiment and the resulting machine trajectories are observed (Fig. 13) to follow the constructed soil geometry. The boom moves upwards significantly so as to follow the soil surface geometry despite the reference trajectory being a static boom.

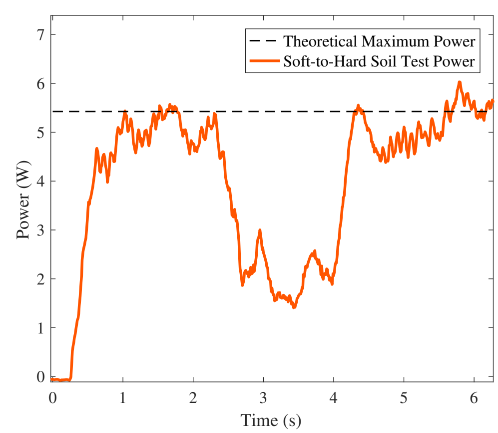

Fig. 12. Power from arm for rig operating in soil which includes an abrupt transition in soil hardness

Preprint submitted to IEEE Robotics and Automation Letters as Submission for RA-L and ICRA
Received September 10, 2018 17:24:52 PST

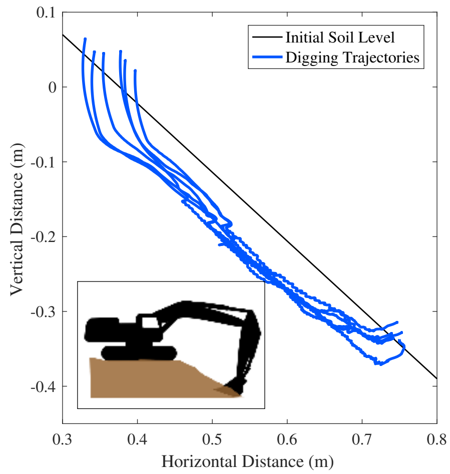

Fig. 13. Multiple trajectories for the excavator digging an angled soil surface. Nominal trajectory has zero boom velocity which would result in the bucket getting stuck.

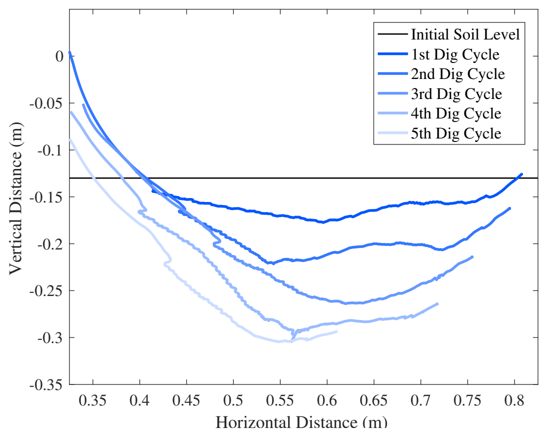

Fig. 14. Excavator digging in successive cycles without restoring the soil environment

5) Multiple Dig Cycles: When digging over multiple cycles (for example while excavating a trench or simply removing large amounts of material) the terrain shape is constantly changing from cycle to cycle and can take irregular geometries. The algorithm follows different paths in every successive cycle so as to excavate a large hole (Fig. 14).

VI. Conclusion and Further Work

The results presented demonstrate that power maximization as a control objective and ESC as a means to achieve this are effective in creating an adaptive digging controller. The resulting algorithm can be combined with other planning strategies to give excavation robots the ability to adapt to changing conditions while maximally utilizing their capabilities to move soil.

From the various tests which were undertaken, we identified avenues for potential further development. One simplification used in this letter (and in much of the excavation literature) is excluding motion of the swing during digging. Expert operators, however, sometimes utilize the swing so as to modulate resistance or follow more complicated soil geometries. For example, if there is an angled bench then the depth varies not only in the radial direction, but also laterally. In this case, probing as proposed in this letter is especially essential. While the effect of vertical motion on bucket load generally follows a known trend (motion upwards generally decreases force and vice versa), the effect of motion in the swing direction on bucket load is unknowable. ESC then allows the excavator to autonomously seek the most advantageous swing motion. Expanding the implementation to include swing actuators would allow this. Additionally, characteristics of the soil learned from one dig cycle could be incorporated into successive dig cycles' trajectory planning, possibly resulting in faster convergence to an optimal state.

References

[1] "Shaping the future of construction," WEF, May 2016.
[2] S. Dadhich, U. Bodin, and U. Andersson, "Key challenges in automation of earth-moving machines," *Autom. Constr.*, vol. 68, pp. 212 – 222, 2016.
[3] S. Singh, "Syntheis of tactical plans for robotic excavation," Ph.D. dissertation, Robotics Institute, Carnegie Mellon Univ., Pittsburgh, June 1995.
[4] A. R. Reece, "Paper 2: The fundamental equation of earth-moving mechanics," pp. 16–22, 1964.
[5] O. Luengo, S. Singh, and H. Cannon, "Modeling and identification of soil-tool interaction in automated excavation," in *Proc. IEEE/RSJ Int. Conf. Intell. Robots Syst.*, vol. 3, Oct 1998, pp. 1900–1906.
[6] H. Cannon and S. Singh, *Experimental Robotics VI*. London: Springer, 2000, ch. Models for automated earthmoving.
[7] S. Blouin, A. Hemami, and M. Lipsett, "Review of resistive force models for earthmoving processes," *J. Aerosp. Eng.*, vol. 14, no. 3, pp. 102–111, 2001.
[8] L. E. Bernold, "Motion and path control for robotic excavation," *J. Aerosp. Eng.*, vol. 6, no. 1, 1993.
[9] N. Hogan, "Impedance control: An approach to manipulation: Part itheory," *J. Dyn. Syst. Meas. Contr.*, vol. 107, no. 1, pp. 17–24, 1985.
[10] G. J. Maeda and D. C. Rye, "Learning disturbances in autonomous excavation," in *Proc. IEEE/RSJ Int. Conf. Intell. Robots Syst.*, Oct 2012, pp. 2599–2605.
[11] A. A. Dobson, J. A. Marshall, and J. Larsson, "Admittance control for robotic loading: Design and experiments with a 1-tonne loader and a 14-tonne load-haul-dump machine," *J. Field Rob.*, vol. 34, no. 1, pp. 123–150, 2017.
[12] D. Jud, G. Hottiger, P. Leemann, and M. Hutter, "Planning and control for autonomous excavation," *IEEE Rob. Autom. Lett.*, vol. 2, no. 4, pp. 2151–2158, Oct 2017.
[13] D. A. Bradley and D. W. Seward, "The development, control and operation of an autonomous robotic excavator," *J. Intell. Rob. Syst.*, vol. 21, no. 1, pp. 73–97, January 1998.
[14] E. McKyes, *Soil Cutting and Tillage*. Amsterdam: Elsevier, 1985.
[15] K. B. Ariyur and M. Kristic, *Real-Time Optimization by Extremum Seeking Control*. New York: John Wiley and Sons, inc, 2003.
[16] M. Guay, "A perturbation-based proportional integral extremum-seeking control approach," *IEEE Trans. Automat. Contr.*, vol. 61, no. 11, pp. 3370–3381, Nov 2016.
[17] I. Vandermeulen, M. Guay, and P. J. McLellan, "Discrete-time distributed extremum-seeking control over networks with unstable dynamics," *IEEE Trans. Control Network Syst.*, 2018, early Access.
[18] G. C. Goodwin and K. S. Sin, *Adaptive filtering prediction and control*. New York: Elsevier, 2009.
[19] ROS. Accessed: 2018-08-01. [Online]. Available: http://www.ros.org/